Title: Synthesis and characterization of copper-alumina metal matrix composite by conventional and spark plasma sintering

Authors: K. Dash, B.C. Ray, D. Chaira

PII: S0925-8388(11)02223-7
DOI: doi:10.1016/j.jallcom.2011.11.136
Reference: JALCOM 25540

To appear in: *Journal of Alloys and Compounds*

Received date: 20-5-2011
Revised date: 25-11-2011
Accepted date: 28-11-2011

Please cite this article as: K. Dash, B.C. Ray, D. Chaira, Synthesis and characterization of copper-alumina metal matrix composite by conventional and spark plasma sintering, *Journal of Alloys and Compounds* (2010), doi:10.1016/j.jallcom.2011.11.136

Graphical Abstract

The evolution of microstructure, density and hardness of Cu-Al_2O_3 metal matrix composites with different techniques of sintering has been demonstrated here. The effect of sintering atmosphere has also been discussed. Synthesis of microcomposites was carried out by reinforcing 5, 10 and 15 volume % of alumina powder particle (average size~5.71μm) in copper matrix via conventional sintering using H_2 and N_2 atmospheres. Nanocomposites of 1, 5, 7 volume % alumina (average size<50nm) reinforced in copper matrix was fabricated by powder metallurgy route using spark plasma sintering technique. These micro- and nano-composites have been characterized by X-Ray diffraction and scanning electron microscopy followed by density and hardness measurements. The fabrication of Cu-Al_2O_3 metal matix microcomposites and nanocomposites via conventional route and spark plasma sintering routes are studied and compared. Maximum Vickers hardness of 60 and 80 are obtained when the Cu-15 volume % Al_2O_3 is conventionally sintered in N_2 and H_2 atmosphere respectively. However, maximum hardness value of 125 is achieved for the Cu-5 vol. % Al_2O_3 nanocomposite prepared by spark plasma sintering. It has been observed that Cu-Al_2O_3 metal matrix composite (MMC) shows poor mechanical properties when it is conventionally sintered in N_2 atmosphere than H_2 atmosphere.

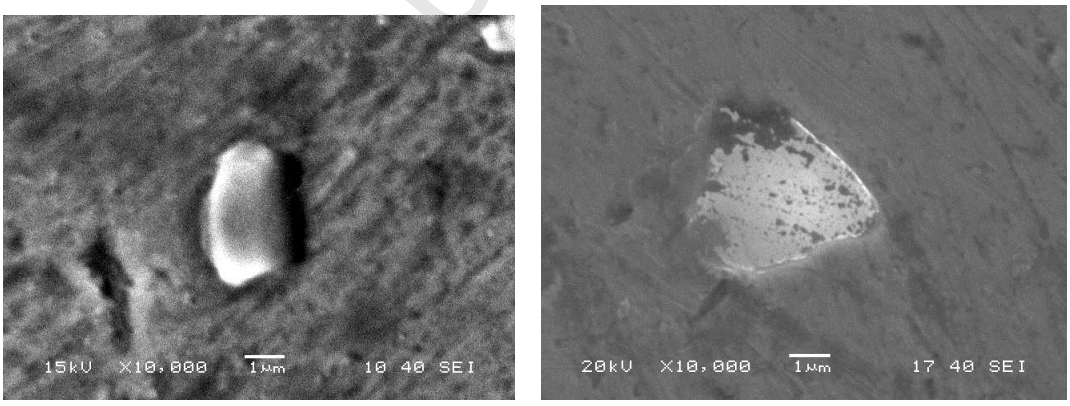

SEM micrograph of Cu-5 vol. % Al_2O_3 MMC sintered in N_2 (left) and H_2 (right) atmosphere

Title – Synthesis and characterization of copper-alumina metal matrix composite by conventional and spark plasma sintering

Authors – Khushbu Dash, Bankim Chandra Ray, Debasis Chaira

Author affiliations –

Corresponding author

Debasis Chaira
Asst. Professor
Dept. of Metallurgical and Materials Engg.
National Institute of Technology,
Rourkela – 769008
Phone – +91-661-2462561(O)
Fax - +91-661-2465999
E-mail – chaira.debasis@gmail.com

Co-authors

Khushbu Dash
Research Scholar
Dept. of Metallurgical and Materials Engg.
National Institute of Technology,
Rourkela – 769008
Phone – +91-9439281130(M)
Fax - +91-661-2465999
E-mail – khushbudash@gmail.com

Bankim Chandra Ray
Professor
Dept. of Metallurgical and Materials Engg.
National Institute of Technology,
Rourkela – 769008
Phone – +91-9437221560 (M)
Fax - +91-661-2465999
E-mail – drbcray@gmail.com

Synthesis and characterization of copper-alumina metal matrix composite by conventional and spark plasma sintering

K. Dash, B.C. Ray and D. Chaira[!]

Department of Metallurgical & Materials Engineering

National Institute of Technology Rourkela, Rourkela – 769008, India

Research Highlights

- Better matrix-reinforcement interfacial bonding and compatibility in hydrogen atmosphere than nitrogen atmosphere.
- An improvement in density and hardness under hydrogen atmosphere than in nitrogen atmosphere is manifested.
- Spark plasma sintering method results in higher density and hardness values than conventional sintering.

Abstract

The evolution of microstructure, density and hardness of Cu-Al_2O_3 metal matrix composites with different techniques of sintering have been demonstrated here. The effect of sintering atmosphere on the interfacial compatibility of matrix and reinforcement has also been discussed. Synthesis of microcomposites was carried out by reinforcing 5, 10 and 15 volume % of alumina powder particles (average size~5.71μm) in copper matrix via conventional sintering using N_2, H_2 and Ar atmospheres. Nanocomposites of 1, 5, 7 volume % alumina (average size<50nm) reinforced in copper matrix were fabricated by powder metallurgy route using spark plasma sintering technique. These micro- and nano-composites have been characterized by X-Ray diffraction and scanning electron microscopy followed by density and hardness measurements. Cu-Al_2O_3 metal matrix micro- and nanocomposites fabricated by conventional and spark plasma sintering routes were studied and compared. Maximum Vickers hardness of 60, 75 and 80 was obtained when the Cu-15 volume % Al_2O_3 was conventionally sintered in N_2, Ar and H_2 atmosphere respectively. However, maximum hardness value of 125 has been achieved for the Cu-5 vol. % Al_2O_3 nanocomposite prepared by spark plasma sintering. It has been observed that Cu-Al_2O_3 metal matrix composite (MMC) shows poor mechanical properties when it is conventionally sintered in N_2 or Ar atmosphere compared to that in H_2 atmosphere.

Keywords: Cu-Al_2O_3; Metal matrix composite; Conventional sintering; Spark plasma sintering; Nanoparticles.

!Corresponding author:
E-mail: chaira.debasis@gmail.com
Phone no: +91 661 2462561

1. Introduction

The physical and mechanical superiority of nano-structured materials has fascinated scientists in recent times [1]. The strengthening due to grain refinement can be delegated to a number of theories such as the Hall-Patch relation, Orowan bowing mechanism, Taylor relationship and several other models [2]. Metal matrix composites (MMCs) combine both metallic properties (ductility and toughness) with ceramic properties (high strength and modulus) possess greater

strength in shear and compression and high service temperature capabilities. The extensive use of MMCs in aerospace, automotive industries and in structural applications has increased over past 20 years due to the availability of inexpensive reinforcements and cost effective processing routes which give rise to reproducible properties [3]. The frontier zone between the matrix and reinforcement phase (interface or interphase) is an essential part of MMC. Bonding between the two phases develops from interfacial frictional stress, physical and chemical interaction and thermal stresses due to mismatch in the coefficients of thermal expansion of the matrix and reinforcement. During the design of a MMC the underlying interfacial phenomenon which governs the transmission of thermal, electrical and mechanical properties is of utmost importance [4].

Copper is an excellent material for electrical applications whose efficiency can be enhanced by improving its mechanical properties [5]. When alumina particles are dispersed in copper matrix, they exhibit unique characteristics, such as high thermal and electrical conductivity, as well as high strength and excellent resistance to annealing [6]. The applications encompass resistance welding electrodes, lead frames and electrical connectors [7]. Its use has been suggested in International Thermonuclear Experimental Reactor (ITER). The first wall of the reactor has been proposed to be made out of austenitic stainless steel plate bonded to an alumina dispersed copper plate. Such critical applications of this material give way to their fabrication by powder metallurgy route.

The technique of consolidation without melting is a boon to the world of materials which is possible by thermal activation of mass transport processes [8]. The driving force for the former being reduction of surface and grain boundary energies, high sintering temperature is a desirable facet for formidable strength [9]. The consolidation of matrix and reinforcement powders is successful when the interfacial bonding along with the uniform distribution and other factors promote good mechanical properties. An important aspect of dispersion strengthening is homogeneous distribution of reinforcement in nanometer scale, and the introduction of as small as possible amount of reinforcement in the matrix metal [10]. Pure copper does pose a threat in terms of mechanical pursuit, such as abrasion, sudden failure due to contact resistance (i.e. because of poor high temperature performance) [11]. Regarding reinforcements, oxide

nanoparticles are most suitable because of their hardness, stability and insolubility in base metal and they also offer obstacles to dislocation motion at elevated temperatures without affecting the electrical and thermal conductivity [10]. The selection of sintering atmosphere for a system is purely system specific. The metals that require protection from oxidation since oxides hinder diffusion bonding and evolution of desired properties need an inert or reducing environment. Control of sintering atmosphere provides ample opportunity to tailor the degree of sintering and the material chemistry [12]. Many sintering atmospheres are used across the globe starting from air, nitrogen, argon, oxygen and hydrogen or the blend of these in desired proportion. But the literature about the effect of sintering atmosphere on the interfacial bonding of matrix-reinforcement for the solid state fabrication of Cu-Al_2O_3 composites is scarce. The effect of sintering atmospheres on the wetting behavior and interfacial bonding of titania and liquid copper was investigated by J. Li [13]. The effect of sintering atmosphere on pore filling of aluminum was studied by Schaffer et al. [14]. In the present study, the sintering of Cu-Al_2O_3 system has been carried out in argon, hydrogen and nitrogen atmosphere but as the vol. % of reinforcement and fabrication route in the existing literature and in our experiments differ, direct comparison is not feasible. Several studies have been conducted, which show the effect of sintering atmosphere on the interface formation and eventually on the microstructural and mechanical properties of the composite. Hence the effect of sintering atmospheres on a particular system needs proper attention. The final product obtained by sintering of copper and alumina powders via conventional route in nitrogen atmosphere can have many deficiencies (in physical attributes, such as poor matrix-reinforcement bonding, poor densification and hardness). The earlier results led our thinking to the role of the sintering atmosphere in our system. The sintering of this system in reducing atmosphere yielded astonishing results to be quantified further. The unification of copper and alumina powders by spark plasma sintering where the alumina particles are in the order of nanoscale, the properties are still better. Yoshino et al. have reported that the pores within the bonding interface can be formed due to the release of oxygen gas in liquid copper, which can also be extended to the solid state [15]. Seager et al. have found that smaller pores may be the result of pull out of Cu_2O particles observed on the alumina fracture surface [16]. The role of oxygen in the bonding of copper and alumina has opposite effects in liquid and solid state fabrications. The presence of oxygen is vital in the case of liquid state bonding and equally undesired in solid state bonding. The state of bonding rests mostly on

the nature of the sintering atmosphere. The spark plasma sintering technique is becoming popular due to the intrinsic advantages of the method and the enhanced material properties, as well as lower processing temperature and shorter sintering time to consolidate powders compared to conventional methods. The differences between SPS and conventional methods include process efficiency and energy savings as well as microstructural and compositional implications. Sintering at lower temperatures and shorter times reduces the threat of vaporization, minimizes grain growth and renders cleaner grain boundary. Spark plasma sintering (SPS) uses high amperage, low voltage, pulse DC current and uniaxial pressure to consolidate powders [8]. The exciting results obtained in the sintering of composites by SPS can be ascribed to the differential activation of the matrix and reinforcement, as the existing theory for SPS proposes that the current pathway is unlike for conducting and non-conducting powders. A combination of current flow through the sample and radiative heat loss on the die wall gives rise to a radial temperature distribution in conductive samples. The studies on copper-alumina MMC along with their properties have been carried out by several groups [17-20]. Fathy et al. [17] have demonstrated improvement in compressive strength, hardness and wear resistance of Cu-Al_2O_3 system, Ritasalo et al. [18] have reported hardness value of 1.58 GPa of SPS sintered Cu-Al_2O_3 composite. The increase in arc erosion resistance of Cu-Al_2O_3 with the increase in alumina content has been reported by Wang et al. [19]. Nachum et al. [20] have studied the microstructural and mechanical properties of Cu-Al_2O_3 nanocomposites fabricated by HIPing, where the increase in strength and nanohardness has been highlighted. The fabrication of Cu-Al_2O_3 nanocomposites containing high volume fraction of alumina by SPS route has been performed by Michalski et al. [21], shows that it does not cater to the cost effectiveness factor of engineering industry. The influence of sintering atmosphere on the matrix-reinforcement bonding and subsequently other properties, such as densification and hardness, has not yet been understood in detail.

The main aim of the present investigation is to study the effect of sintering atmospheres and sintering techniques on the microstructure and mechanical properties of Cu-Al_2O_3 composite. The differential behaviour of copper and alumina at different sintering temperatures and atmospheres lead to differences in development of microstructures, which eventually control the

properties of the composite. The differences in microstructures and properties of Cu-Al_2O_3 fabricated by conventional and spark plasma sintering techniques has been studied here.

2. Experimental

The as-received copper (Loba Chemie, purity > 99.7%, average size-11.09μm) and alumina (Sigma Aldrich, average size-5.71μm and <50 nm) powders were mixed and blended separately using agate mortar for 60 minutes to ensure homogeneous mixing. Alumina powders of both sizes were mixed with copper powder to prepare the samples. Copper and 5, 10, 15 volume % of alumina powders were compacted into cylindrical pellets (diameter: 15 mm) using uniaxial hydraulic press at an applied pressure of 700 MPa for 2 minutes. The green samples were then sintered by conventional sintering in a tubular furnace at 900°C for a holding time of 60 minutes in nitrogen (Asiatic gases Ltd., 99.8% purity) atmosphere at a heating rate of 5°C/minute. In another set of experiment, specimens of same constituents were fabricated by sintering them in hydrogen (99% purity) atmosphere, keeping the other parameters fixed. The third set of specimens with similar composition as above was synthesized by sintering in argon atmosphere (British oxygen company, 99.994% purity), keeping rest of the parameters constant.

Nanocomposites containing 1, 5 and 7 vol. % of Al_2O_3 (average size<50nm) and copper were fabricated by mixing the matrix and reinforcement powders, followed by spark plasma sintering (SPS) (DR SINTER LAB SPS Syntex). The temperature for SPS was 700°C at a pressure of 50MPa for 5 minutes under vacuum at a heating rate of 80°C/minute. The densification of all the specimens was estimated using Archimedes method. The as-received copper and alumina powders were characterized by particle size analyzer (MALVERN Mastersizer 2000) while sintered specimen were characterized by using X-Ray diffractometer (PANalytical model: DY-1656, CuKα radiation) and scanning electron microscope (JEOL 6480 LV). The micrographs of the specimen were obtained by chemically etching the samples by a mixture of 5 g $FeCl_3$ and 50 ml HCl in 100 ml distilled water. The micro-hardness values of all the specimens were determined by Vickers hardness tester (Leco LV 700) applying a load of 0.3 kgf for a dwell time of 1 sec. The readings were recorded here at four equivalent locations for each specimen.

3. Results and discussion

3.1 X-Ray diffraction

The X-Ray diffraction of sintered samples was carried out to study the phases present. The alumina peaks confirm to be monoclinic in nature. The X-Ray diffraction patterns of the specimen sintered conventionally in nitrogen, hydrogen and argon atmosphere, illustrated in Figs. 1(a), (b) & (c) show the presence of cuprous oxide (Cu_2O) along with Cu and Al_2O_3 in all the cases. In the composites sintered in argon atmosphere the peak for cuprous oxide is not that intense, but the presence of oxygen has been further verified by EDS. Fig. 1(d) reveals the presence of copper as well as alumina; as the alumina content in the nanocomposites is minimal, the alumina peaks are not distinct and clear. The composites fabricated by SPS route do not show any peak of cuprous oxide as sintering was carried out in vacuum atmosphere.

3.2 Scanning electron microscopy

The microstructures obtained by scanning electron microscope (SEM) give ample information about the pore density, distribution, alignment and nature of pores along with the matrix-reinforcement bonding. Figs. 2(a), (b) & (c) depict the microstructures of Cu-Al_2O_3 MMC, where white patches correspond to alumina and the grey area referring to the copper matrix. The scanning micrographs illustrated in Figs. 2(a), (b) & (c) reveal a clear difference between the bonding of copper and alumina in N_2, Ar and H_2 atmospheres. The specimen sintered in hydrogen atmosphere, (Fig. 2(b)), shows good copper-alumina interfacial bonding, as compared to the composites sintered in nitrogen and argon atmosphere, (Figs. 2(a) & (c)). There is an existence of discontinuity in bonding between alumina particles and the copper matrix when the composites sintered in argon atmosphere (Fig. 2(c)). The proximity and degree of physical attachment of the alumina and copper particles in the sintered composites can be ranked in order of nitrogen, argon and hydrogen (in increasing order). It is desirable to remove cuprous oxides from the interface of Cu-Al_2O_3 composite to enhance mechanical properties. This fact can be attributed to the high bond strength of Cu/Al_2O_3 than those of Cu_2O/Al_2O_3 and Cu/Cu_2O [15, 22, and 23]. This could possibly be attributed to the formation of cuprous oxide at low temperatures (tentatively 700°C) and the possibility of onset of decomposition at higher temperatures close to 1000°C. The decomposition yields copper and oxygen; where the oxygen escapes from the surface creating voids and expanding them eventually. The creation of voids impedes the densification causing swelling in addition to the oxygen released from the copper oxide formed

at the copper-alumina interface disturbs the continuity in bonding of copper and alumina. Ghasemi et al. have reported that in reducing atmosphere the Cu_2O particles will be reduced to Cu and the removal of Cu_2O particles from the interface results in the substitution of Cu_2O/Al_2O_3 and Cu/Cu_2O interfaces by a Cu/Al_2O_3 interface [24]. Chiang et al. [22] and Sun, Discoll [25] have shown that the strength of Cu/Al_2O_3 interface is higher than that of Cu_2O/Cu interface. Therefore, an improved alumina-copper contact surface and a decreasing stress concentration owing to the absence of Cu_2O particles resulted in an increase of bond strength. The micrographs in Figs. 3(a), (b) & (c) also depict the fact that as the alumina content increases the tendency of embedment of alumina particles in the copper matrix deteriorates. Elements with less stable oxides than alumina will remain reactive only to the extent of obtaining oxygen from the atmosphere [26]. The EDS analysis of the specimen (the whole micrograph in Figs. 3(a), (b) & (c) was selected for EDS analysis) sintered in nitrogen, hydrogen and argon atmosphere is shown in Figs. 3(a), (b) & (c) which shows a noticeable difference in the oxygen content of the samples. The elemental composition of oxygen estimated in Cu-15 vol. % Al_2O_3 MMC sintered in N_2, H_2 and Ar atmosphere is 21.02, 4 and 12.99 wt % respectively. It is evident from the EDS values that a smaller amount of O_2 is present in the composite sintered in H_2 compared to that in N_2 atmosphere. The amount of oxygen present in the specimens sintered in argon atmosphere is somewhere in between of that of nitrogen and hydrogen. The microstructure in Fig. 4 reveals that the distribution of the alumina particles is almost uniform in nanocomposites. The distribution of alumina particles in nanocomposites appears to be better than that in microcomposites. The agglomeration of alumina nanoparticles with higher volume percent of it is inevitably higher as shown in Fig. 5(c) as compared to those in Figs. 5(a) & (b). An increase in specific surface area (as number of nanoparticles increases) leads to higher inter-particle friction and thus leading to decreased particle distribution [27]. This is due to high surface energy of high volume % reinforcement nanoparticles.

The nature of porosity varies with the variation of volume % of alumina. The composite having 1 vol. % alumina shows isolated pores, whereas 5 vol. % alumina shows interconnected pores, as shown in Figs. 5(a) & (b). The interconnected pores in nanocomposites sintered by SPS exist because alumina nanoparticles possess hardness and also give rise to the problem of agglomeration [27]. The presence of interconnected pores in nanoscale, have a positive attribute to the mechanical performance of the nanocomposite. Twin boundaries can also be seen in Fig. 6

(7 volume % of alumina reinforced nanocomposite), which might have occurred due to high internal strain and high temperature while sintering i.e. a rise in temperature within a short period of time. The presences of twins indicate a low mobility of dislocations, which directs the good mechanical value of the composite [28]. The Back scattered electron (BSE) image shows diminished grain growth of copper in the areas where the distribution is proficient due to the pinning effect of the nanosized alumina particles [29]. In nanocomposites, as the interparticle distance decreases, interaction between the dislocations and particles increases, and this results in faster dislocation multiplication. The matrix-reinforcement bonding seems to have improved in the nanocomposites sintered by SPS. The reason could be anticipated as the high surface energy of the particles compelling them to compensate their thermodynamic instability by efficient bonding.

3.3 Density measurement

The densities of all the specimens recorded using Archimedes method shown in Fig. 7(a) indicates that the composites sintered by conventional method in nitrogen atmosphere show a slight increase in densification with increasing alumina content. With the increasing amount of finer particles (alumina particles are finer than copper particles), the particle packing and particle–particle contact increases, which leads to higher density. The density of composites sintered in argon increases up to 10 vol. % of alumina and then it decreases slightly. This could be supported by the fact that as the amount of alumina increases to 10% there is some chemical interfacial phenomenon taking place at this particular composition [30] which can be further confirmed by high resolution electron microscope. The trend in densification for the compacts sintered in hydrogen atmosphere is opposite to that obtained in the nitrogen atmosphere, which needs further study to be clarified. The amount of cuprous oxide (Cu_2O) formed in H_2 atmosphere is less as compared to that in N_2 atmosphere. The composites sintered in nitrogen atmosphere have considerably low density due to the fact that during decomposition of cuprous oxide, oxygen gets released expanding the sintered compact by creating voids. The density of composites sintered by spark plasma sintering technique is quite high (Fig. 7(b)). The agglomeration problem of nanoparticles leads to lesser densification in nanocomposites where as the problem of agglomeration does not impair the densification of microcomposites to a larger

extent. This is due to the fact that the specific surface of coarser particles is lower and the powder compressibility is higher [24].

3.4 Hardness study

The hardness of microcomposites sintered in nitrogen as well as hydrogen atmosphere shown in Fig. 8(a), indicate that the microcomposites sintered in hydrogen atmosphere show higher hardness values than those sintered in nitrogen atmosphere. The microcomposites sintered in argon atmosphere possess hardness values close to that of nitrogen atmosphere. The underlying fact can be correlated with the densification study: the density is higher for the microcomposites sintered in hydrogen atmosphere, which complements the hardness data. The proposed reason possibly could be the basis of argument in the comparison of hardness profiles of microcomposites. The trend of hardness values shown by the nanocomposites is illustrated in Fig. 8(b). The above behavior shows an increase upto 5 vol. % alumina and then a fall in the hardness value for 7 vol. % alumina. The 7 vol. % alumina composition may facilitate higher degree of agglomeration of alumina nanoparticles but till 5 vol. % alumina the agglomeration seems to be insignificant. This can be anticipated as the surface of the agglomerated particle (in case of 5 vol. %) may not be sufficiently large enough to disturb and deviate the close intimacy at the particle-matrix interface. This could be a possible reason in attributing insignificant deteriorating effect on the hardness value which is visible in Fig. 8(b). Another reason for having a positive effect of alumina on hardness upto 5 volume % followed by a negative effect could be ascribed to the effective dispersion strengthening till 5 volume % of alumina [28]. Shehata et al. [31] have investigated the hardness values of Cu-Al_2O_3 nanocomposites sintered by conventional method and have reported the average microhardness value for 5% alumina reinforced Cu-Al_2O_3 composite as 67.8 HV, whereas in the present study, nanocomposites fabricated by SPS method produce an average of 124.5 HV for the same composition. The effective dispersion up to 5% of reinforcement also projects an idea about the small-scale pinning in nanocomposites, which prevents grain growth and hence the hardness values are high [32].

4. Conclusion

The Cu-Al_2O_3 microcomposites were fabricated successfully using conventional sintering route in nitrogen, argon and hydrogen atmospheres. The densification process is more efficient in the case of hydrogen than in nitrogen or argon atmosphere. The microstructure of the composites sintered in hydrogen atmosphere reveals better matrix-reinforcement bonding. The problem of poor interfacial bonding in nitrogen and argon atmosphere has been addressed up to a certain extent using hydrogen atmosphere. The EDS analysis also proves the same. The formation of Cu_2O during sintering in nitrogen and argon atmosphere reduced the extent of bonding of copper with alumina. The density and hardness values are also in accordance to the above fact. The poor bonding between copper and alumina particles lead to inefficient load transfer during mechanical loading of the composite. The Cu-Al_2O_3 nanocomposites containing up to 5 vol. % of alumina have been fabricated successfully using spark plasma sintering method. The properties of nanocomposites have been studied to infer that the nanocomposites have superior properties than the microcomposites. The microstructures of these specimens also point towards the above fact.

Acknowledgement

The authors would like to thank the National Institute of Technology (NIT), Rourkela for providing the necessary financial and infrastructural supports. The authors are also grateful to Prof. Bikramjit Basu, Laboratory of Biomaterials, Indian Institute of Technology, Kanpur for coordinating the preparation of samples using Spark Plasma Sintering facility.

References

[1] S. Choi, H. Awaji, Sci. Technol. Adv. Mater. 6 (2005) 2-10.

[2] Y. Li, Y.H. Zhao, V. Ortalan, W. Liu, Z.H. Zhang, R.G. Vogt, N.D. Browning, E.J. Lavernia, J.M. Schoenung, Mat. Sci. Eng. A 527 (2009) 305-316.

[3] S.C. Tjong, Z.Y. Ma, Mat. Sci. Eng. 29 (2000) 49-113.

[4] S. Vaucher, O. Beffort, MMC-Assess Thematic Network, EMPA-Thun, volume 9.

[5] G. Celebi Efe, T. Yener, I. Altinsoy, M. Ipek, S. Zyetin, C. Bindal, J. Alloys Compd. 509 (2011) 6036–6042.

[6] M.S. Motta, P.K. Jena, E.A. Brocchi, I.G. Solorzano, Mat. Sci. Eng. C 15 (2001) 175-177.

[7] H. Nishi, T. Araki, M. Eto, Fusion Eng. Des. 505 (1998) 39–40.

[8] Z.A. Munir and Dat V. Quach, J. Am. Ceram. Soc. 94 (2011) 1–19.

[9] M.T. Luke, Master of Science Thesis in Materials Science and Engineering, Boise State University, May 2010.

[10] M. Korac, Z. Kamberovic, M. Tasic, M. Gavrilovski, Chem. Ind. Chem. Eng. Q 14 (2008) 215-218.

[11] Copper Development Association, Copper in electrical contacts, Technical note (edited version of an original script commissioned by Copper Development Association from H. W Turner and C. Turner of ERA Technology Ltd., Leatherhead, Surrey) 23 (1980).

[12] R. German, Sintering theory and practice, John Wiley and Sons, Inc, New York, 1996, p.421-447.

[13] J. Li, Mater. Lett. 62 (2008) 2110-2113.

[14] G. B. Scaffer, B. J. Hall, S. J. Bonner, S. H. Huo, T. B. Sercombe, Acta Mater. 54 (2006) 131-138.

[15] Y. Yoshino, J. Am. Ceramic Soc. 72 (1989) 1322-1327.

[16] C.W. Seager, K. Kokini, K. Trumble and M.J.M. Krane, Scr. Mater. 46 (2002) 395-400.

[17] A. Fathy, F. Shehata, M. Abdelhameed, M. Elmahdy, Mater. Des. (2011) doi: 10.1016/j.matdes.2011.10.021.

[18] R. Ritasalo, X.W. Liu, O. Soderberg, A. Keski-Honkola, V. Pitkanen, S-P. Hannula, Procedia Engineering 10 (2011) 124-129.

[19] S. Nachum, N.A. Fleck, M.F. Ashby, A. Colella, P. Matteazzi, Mat. Sci. Eng. A 527 (2010) 5065–5071.

[20] X. Wang, S. Liang, P. Yang, and Z. Fan, J. Mater. Eng. Perform. 19 (2010)1330–1336.

[21] Michalski, J. Jaroszewicz, M. Rosinski, D. Siemiaszko and K.J. Kurzydlowski, Solid State Phen 114 (2006) 227-232.

[22] W.L. Chiang, V.A. Greenhut, D.J. Shanefield, L.A. Johnson, R.L. Moore, Ceramic Engg. Sci. Proc 14 (1993) 802-812.

[23] K.P. Trumble, Acta Metall. Mater 40 (1992) 105-110.

[24] H. Ghasemi, M.A. Faghihi Sani, A.H. Kokabi and Z. Riazi, Transaction B: Mechanical Engineering 16 (2009) 263-268.

[25] Y.S. Sun, J.C. Discroll, IEEE Trans Electron Devices, ED-23 (1976) 961-967.

[26] A.G. Metcalfe, Interfaces in metal matrix composites, volume 1 (1974) Academic Press, New York, pp.72-73.

[27] M. Rahimian, N. Parvin, N. Ehsani, Mat. Sci. Eng. A 527 (2010) 1031-1038.

[28] M. Korac, Z. Kamberovic, Z. Andjic, M. Filipovic, M. Tasic, Sci. Sinter 42 (2010) 81-90.

[29] Z. Razavi Hesabi, A. Simchi, S.M. Seyed Reihani, Mat. Sci. Eng. A 428 (2006) 159-168.

[30] A. Upadhyaya, G.S. Upadhyaya, Mater. Des. 16 (1995) 41-45.

[31] F. Shehata, A. Fathy, M. Abdelhameed, S.F. Moustafa, J. Alloys Compd. 476 (2008) 300-305.

[32] S.S. Razavi-tousi, R. Yazdani-Rad, S.A. Manafi, Mat. Sci. Eng. A 528 (2011) 1105-1110.

Figure captions

Fig. 1: XRD diffraction patterns of microcomposites sintered conventionally in (a) nitrogen (b) hydrogen (c) argon atmosphere (d) nanocomposites sintered by spark plasma sintering.

Fig. 2: SEM micrographs of Cu-5 vol. % Al_2O_3 sintered under (a) nitrogen, (b) hydrogen and (c) argon atmosphere respectively.

Fig. 3: SEM micrographs and EDS analysis of Cu-15 vol. % Al_2O_3 sintered in (a) nitrogen, (b) hydrogen and (c) argon atmosphere respectively.

Fig. 4: SEM micrograph of Cu-5vol. % Al_2O_3 nanocomposite sintered by SPS.

Fig. 5: SEM micrographs of (a) Cu-1 vol. % Al_2O_3 (b) Cu-5 vol. % Al_2O_3 (c) Cu-7 vol. % Al_2O_3 nanocomposites sintered by SPS.

Fig. 6: SEM (BSE) micrograph of 7% alumina reinforced Cu-Al_2O_3 nanocomposite sintered using SPS.

Fig. 7: Densification plots for (a) Cu-Al_2O_3 microcomposites and (b) Cu-Al_2O_3 nanocomposites fabricated using conventional and spark plasma sintering respectively.

Fig. 8: (a) Comparison of hardness for Cu-Al_2O_3 microcomposites and (b) Cu-Al_2O_3 nanocomposites fabricated using conventional and spark plasma sintering respectively.

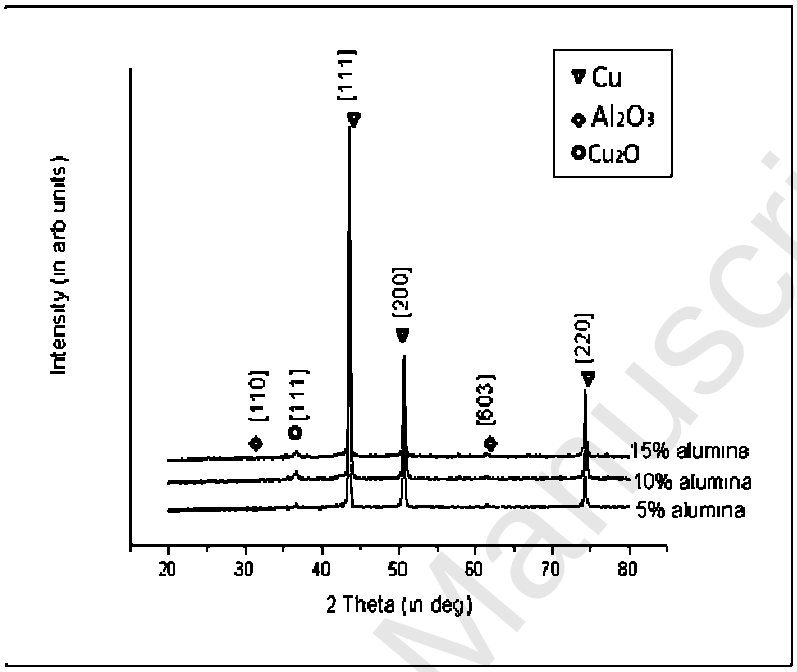

Fig. 1(a)

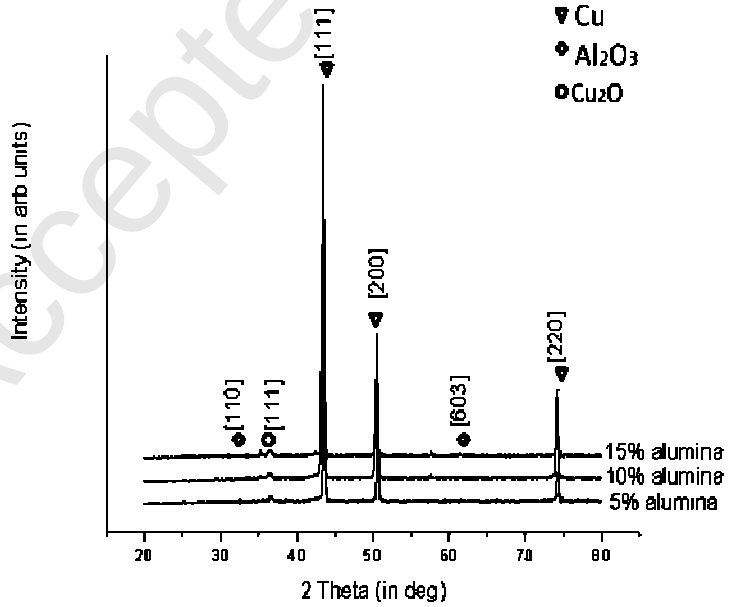

Fig. 1(b)

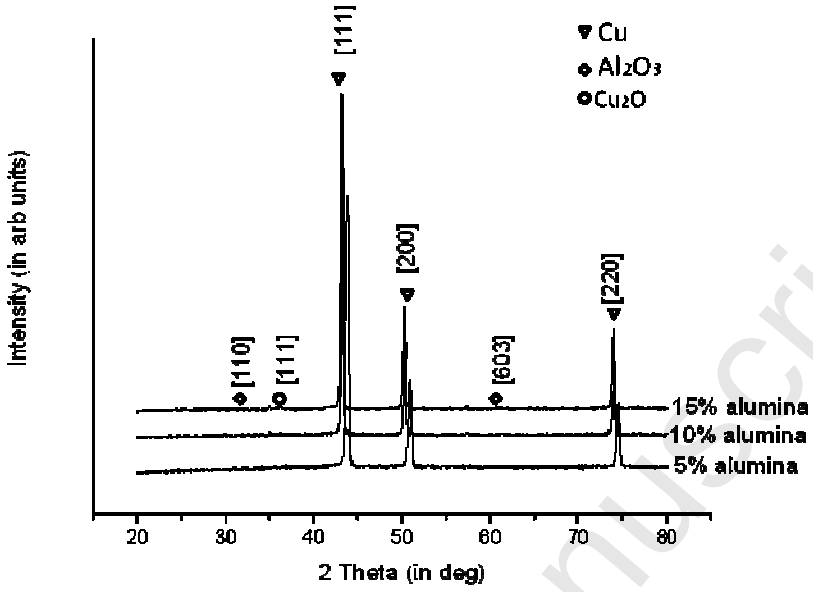

Fig. 1(c)

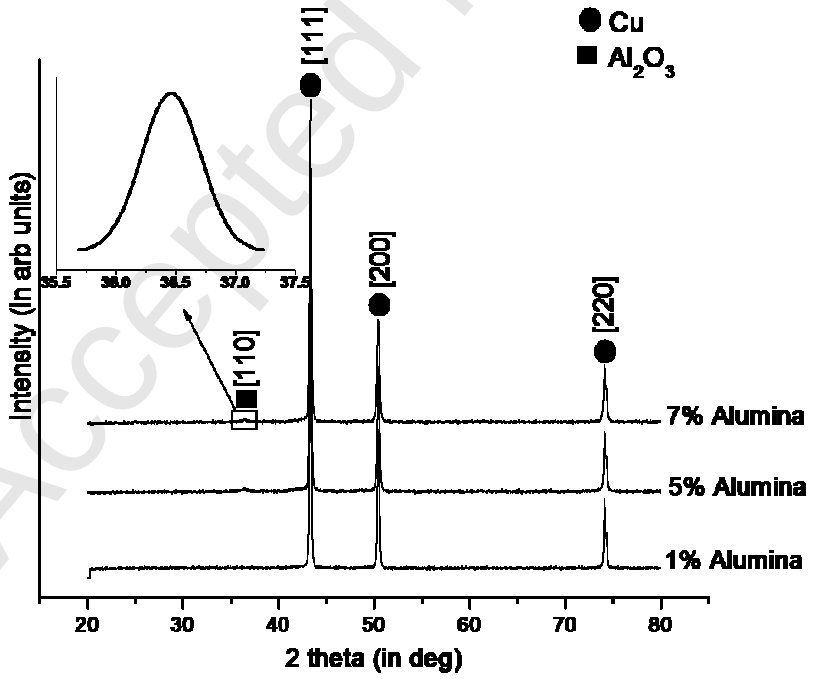

Fig. 1(d)

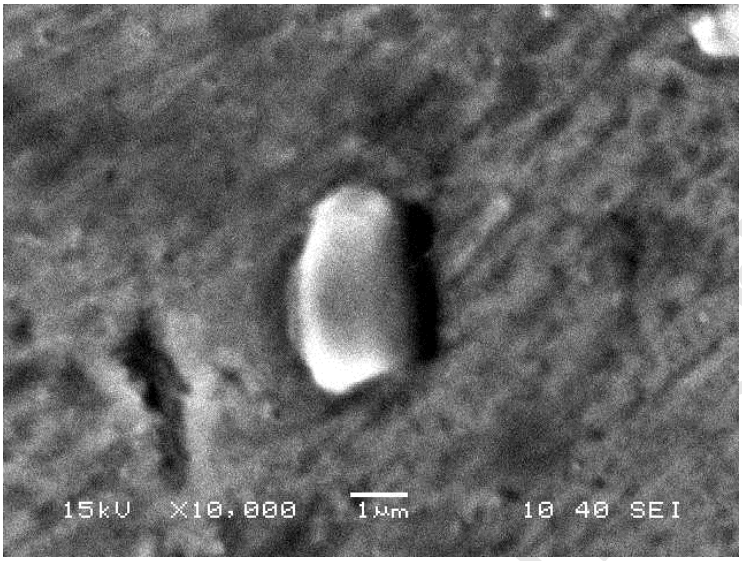

Fig. 2(a)

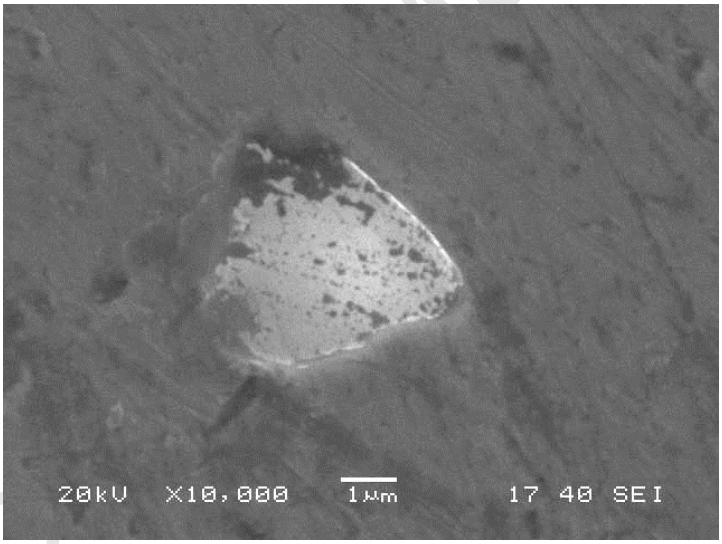

Fig. 2(b)

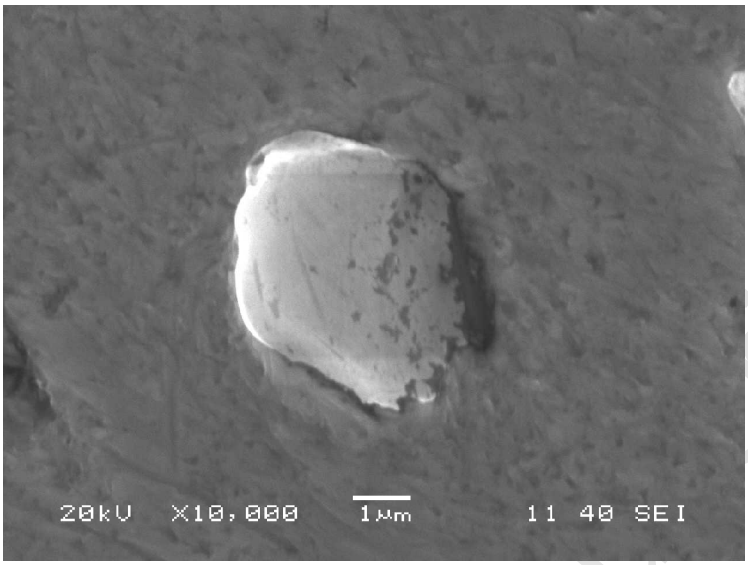

Fig. 2(c)

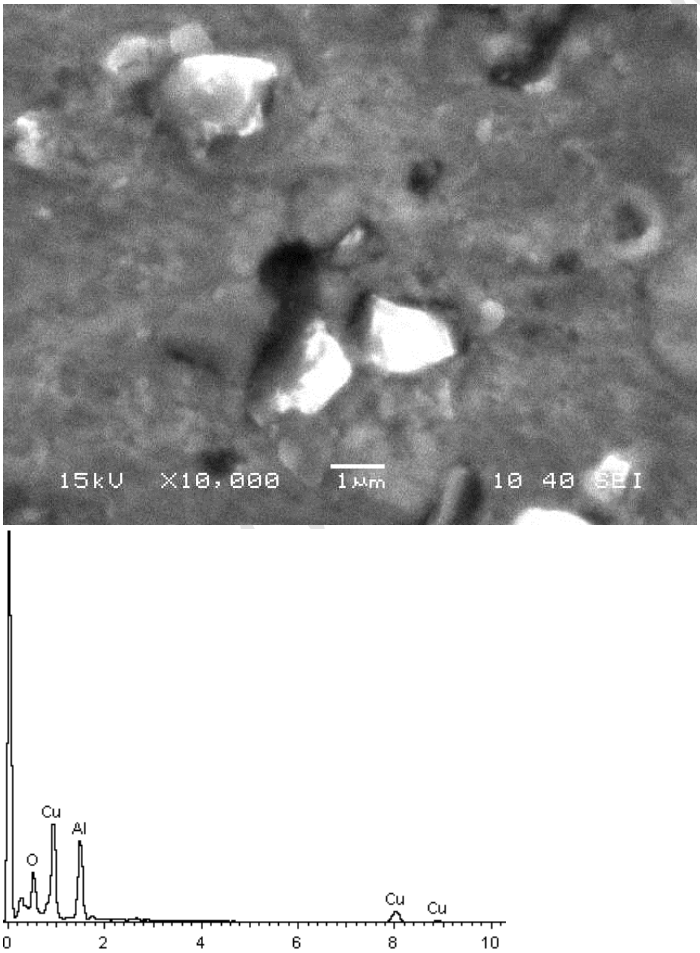

Fig. 3(a)

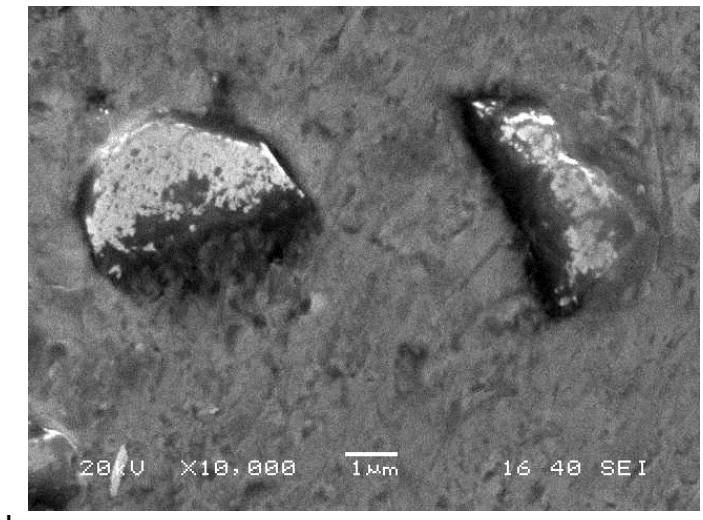

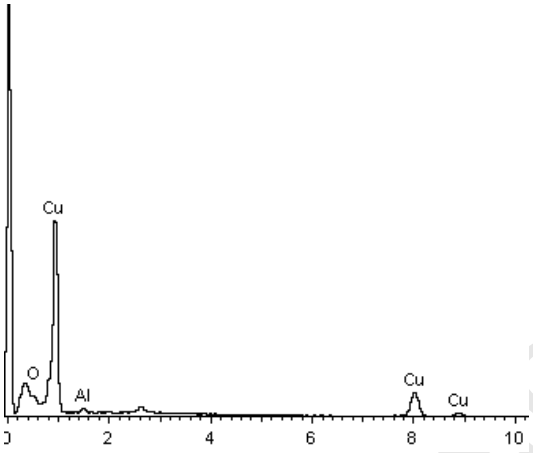

Fig. 3(b)

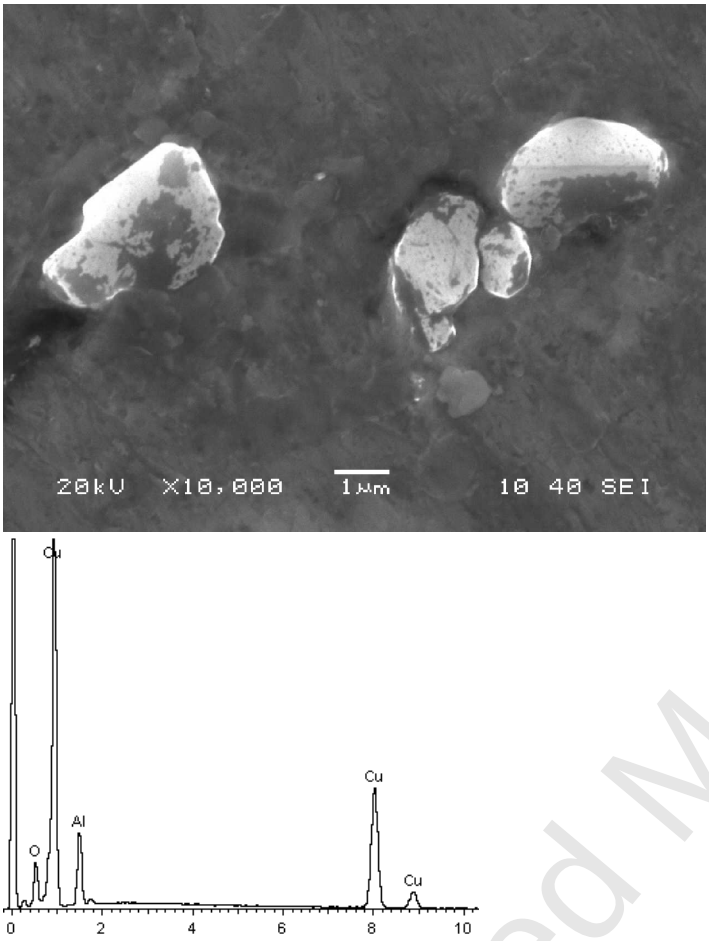

Fig. 3(c)

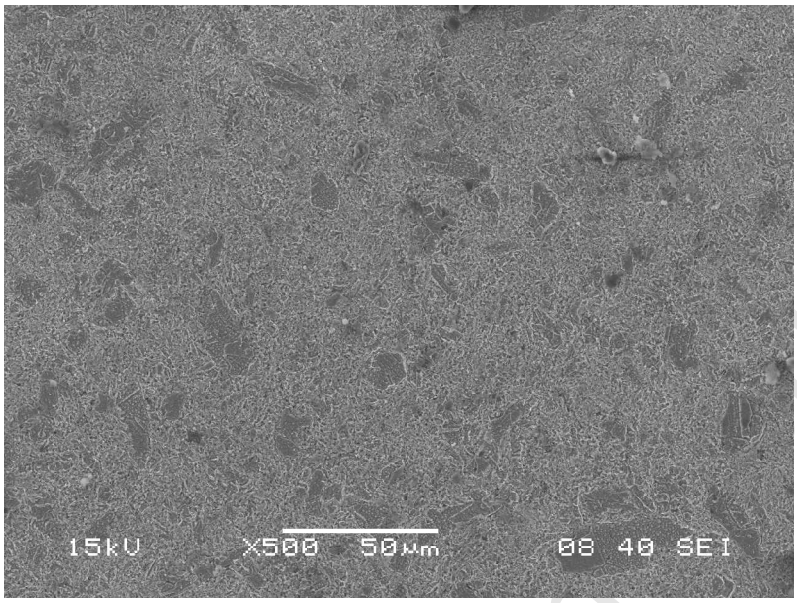

Fig. 4

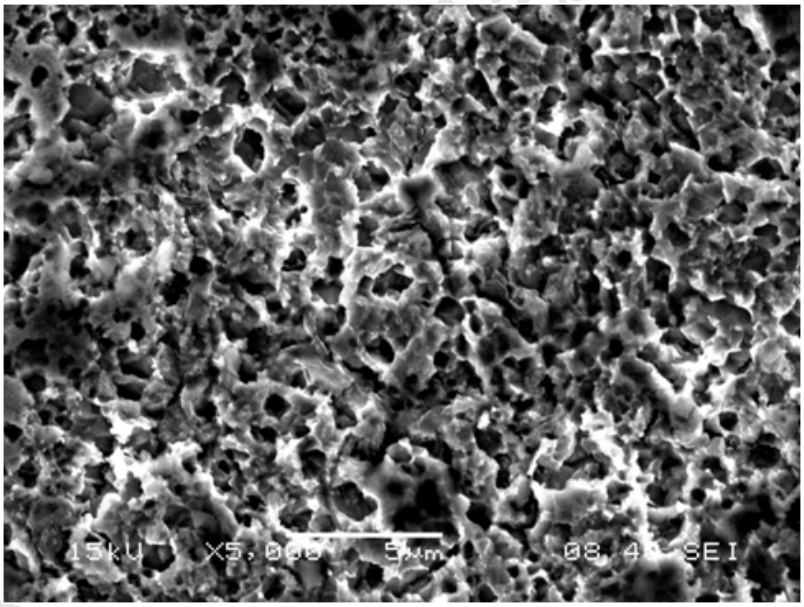

Fig. 5(a)

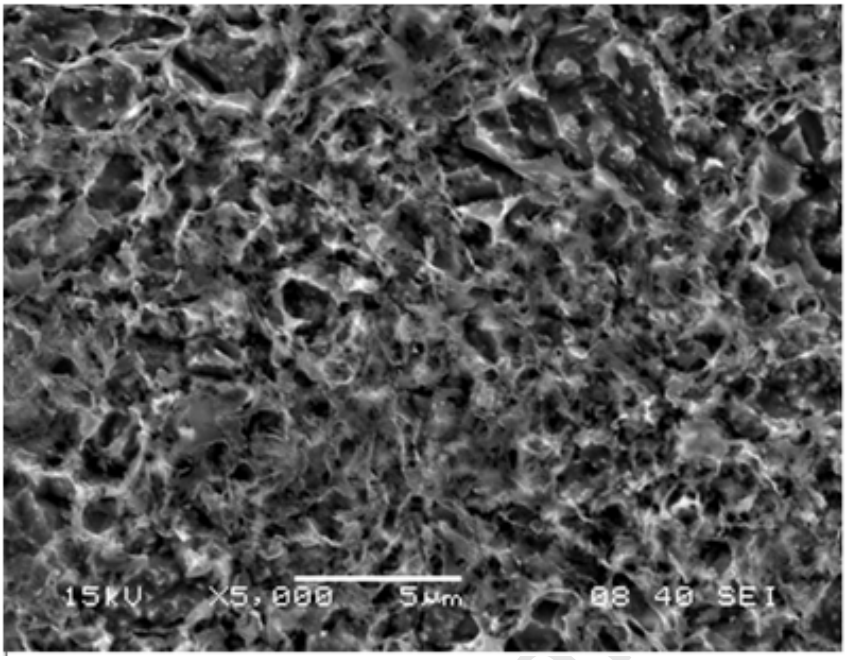

Fig. 5(b)

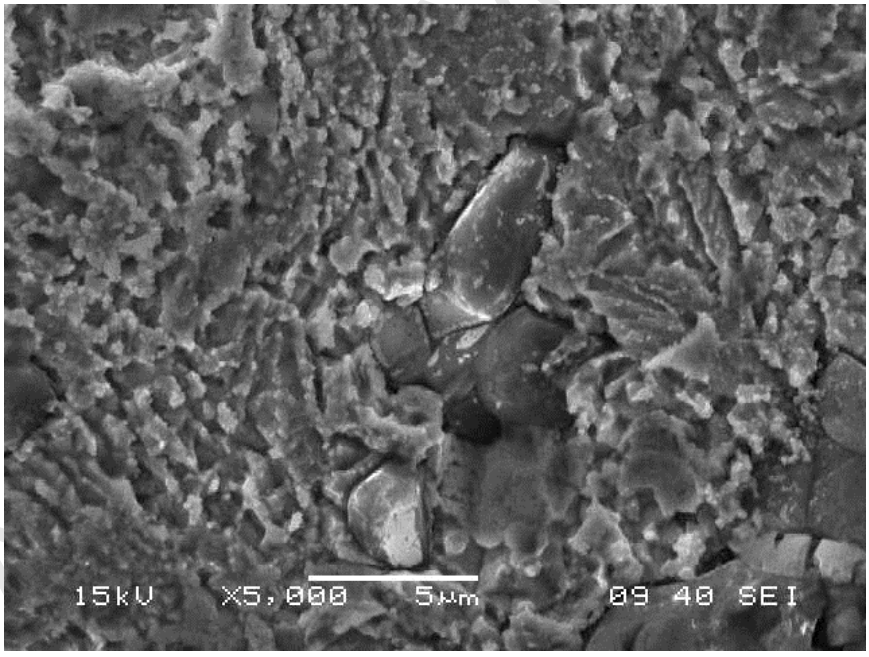

Fig. 5(c)

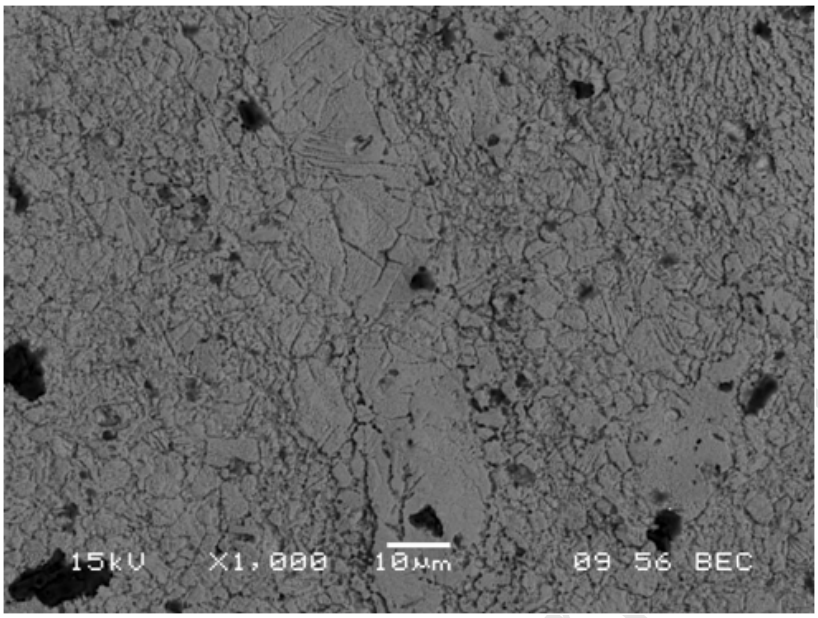

Fig. 6

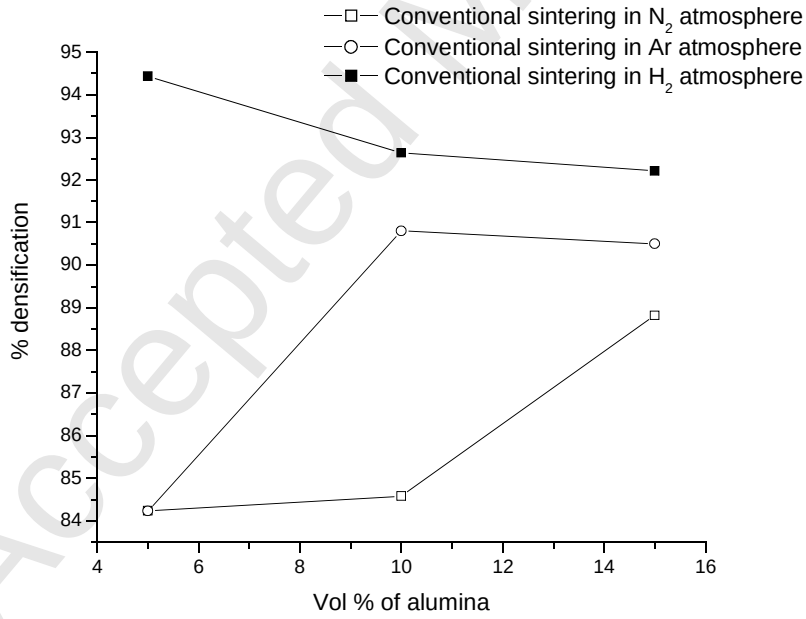

Fig. 7(a)

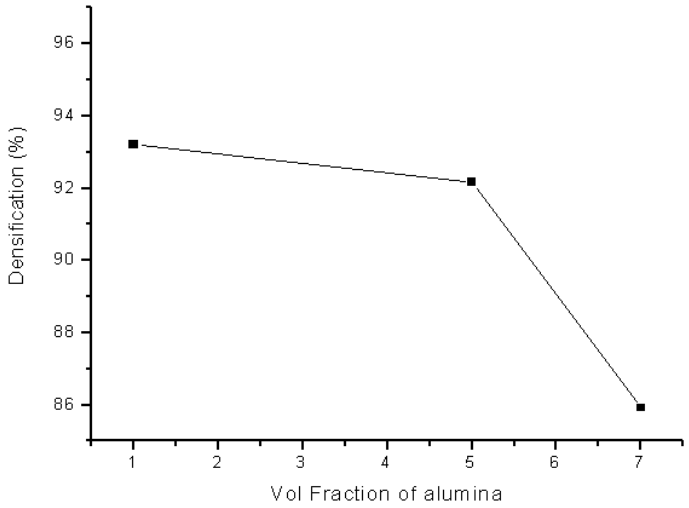

Fig. 7(b)

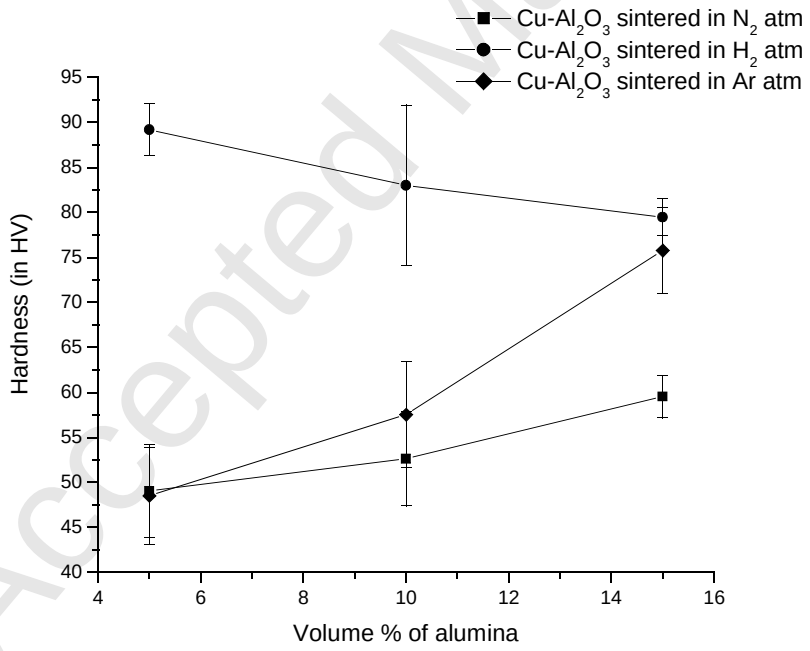

Fig. 8(a)

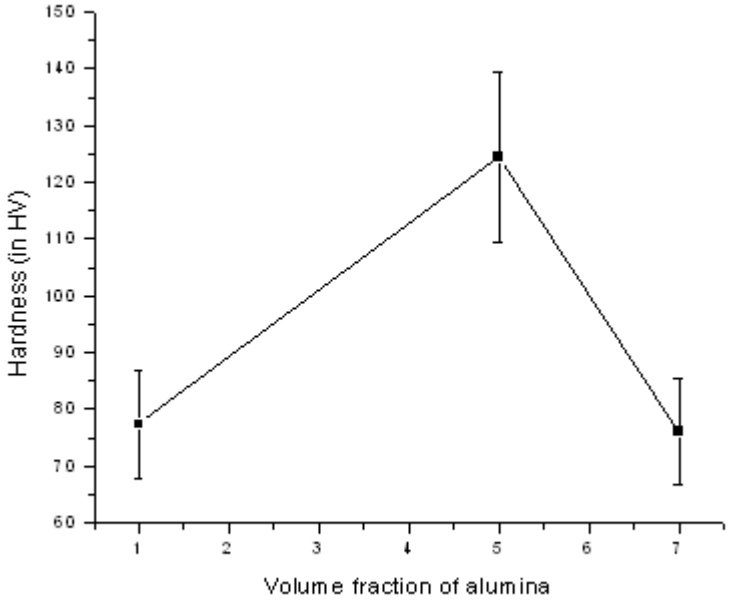

Fig. 8(b)